

Reactivity studies of a soluble LiH-complex and non-spectator behaviour of its stabilising phosphinoamide ligand†

Cite this: *Dalton Trans.*, 2014, **43**, 7078

Andreas Stasch*

We have investigated and compared the reactivity of the phosphinoamide stabilized hydrocarbon-soluble LiH complex $[(\text{LLi})_4(\text{LiH})_4]$ **1** ($\text{L} = [\text{Ph}_2\text{PNDip}]$, $\text{Dip} = 2,6\text{-}^i\text{Pr}_2\text{C}_6\text{H}_3$) and the lithium phosphinoamide $[\text{LLi}]$ **2** towards some unsaturated organic substrates. The complexes $[(\text{LSiMe}_2\text{OLi})_2(\text{HDCCLi})_2]$ **3** ($\text{DCC} = \text{CyNCNCy}$, $\text{Cy} = \text{cyclohexyl}$) and $[(\text{HDCC})_6\text{Li}_8\text{O}]$ **4** were obtained from reactions of **1** with DCC, and the complexes $[\{\text{LN}(\text{Ph})\text{N}(\text{Ph})\text{Li}\}_2]$ **5** and $[\{\text{PhN}(\text{Li})\text{-N}(\text{Li})\text{Ph}\}_4]$ **7** were obtained from reactions of **1** with azobenzene. Complex **5** was furthermore obtained in good yield from **2** and azobenzene, and was converted to the solvate $[\text{LN}(\text{Ph})\text{N}(\text{Ph})\text{Li}(\text{THF})]$ **6**. Complex **7** could be independently synthesized from lithium metal and azobenzene. Complex **1** undergoes hydrolithiation reactions with some substrates, as evidenced by the formation of complexes **3**, **4**, and indirectly by **7**, but also takes part in addition reactions of the stabilizing phosphinoamide ligand onto substrates as shown by the isolation of complexes **3** and **5**. The crystal structures of complexes **3**, **5**, **6**, **7** and $[\text{LLi}(\text{THF})_3]$ are reported.

Received 6th August 2013,
Accepted 25th February 2014

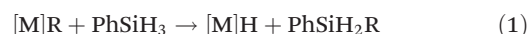
DOI: 10.1039/c3dt52140k

www.rsc.org/dalton

Introduction

Metal hydrides from elements across the periodic table show very different properties and polarity of their hydrogen atoms.¹ Metal hydrides of the s-block metals, *i.e.* groups 1 and 2 of the periodic table except hydrogen, are predominantly saline hydrides with dominant $\text{M}^{n+}\cdots\text{H}^-$ ionic interactions and generally have large lattice energies for their parent solids.^{2,3} Well-defined molecular metal-hydride complexes of the s-block metals and their further chemistry² are still underrepresented compared with those from other parts of the periodic table, despite great interest owing to potential widespread uses in synthesis, catalysis and hydrogen storage applications. This area of chemistry has, however, recently gained popularity because suitable stabilizing ligands are being studied and convenient synthetic routes into s-block metal hydride fragments are now available.² Amongst them, the silane method is convenient and most widely used.^{2,4} Here, a metal alkyl or amide fragment reacts with a silane, often the commercially available phenylsilane, PhSiH_3 , to form a metal hydride fragment and a substituted silane in a metathesis reaction, according to the

general eqn (1); $\text{R} = \text{alkyl or substituted amide}$, $[\text{M}] = \text{s-block metal complex fragment}$.



Suitable stabilizing ligands that chelate and/or sterically protect, and thus generally kinetically stabilize the metal hydride complex from decomposition reactions, are crucial for the development of well-defined complexes. These suppress or prevent the decomposition *via* ligand rearrangement reactions and the generally favoured precipitation of insoluble inorganic metal hydrides, *i.e.* MH or MH_2 , with high lattice energies.

Most structurally characterized examples of s-block metal hydride complexes feature ligand-stabilized metal hydrides involving the group 2 metals, mainly magnesium.² Much less is known about well-defined molecular group 1 metal hydride complexes, and some rare Li^{I} cluster complexes with interstitial hydride^{5,6} and the structurally characterized superaggregate $[(t\text{BuOLi})_{16}(\text{LiH})_{17}]^7$ have been reported. Recently, we used the new sterically demanding phosphinoamide (phosphanyl-amide)⁸ $[\text{Ph}_2\text{PNDip}]^-$ ($\text{Dip} = 2,6\text{-}^i\text{Pr}_2\text{C}_6\text{H}_3$, $\equiv \text{L}^-$, in the stabilization of the novel hydrocarbon-soluble LiH complex $[(\text{LLi})_4(\text{LiH})_4]$ **1**, see Chart 1, which was prepared from the mixed phosphinoamido alkyl complex $[\text{L}_2\text{Li}_4n\text{Bu}_2]$ and phenylsilane according to eqn (1), and studied its properties and reactivity towards benzophenone.⁹ Very recently, we have extended this synthetic concept to isolate well-defined pyrazolato-stabilised hydride-rich LiH clusters with inorganic cores in the nanometer region, for example $[(\text{pz})_{12}\text{Li}_{37}\text{H}_{25}]$ and

School of Chemistry, Monash University, PO Box 23, Melbourne, Victoria 3800, Australia. E-mail: Andreas.Stasch@monash.edu

† Electronic supplementary information (ESI) available: For crystallographic data in CIF. CCDC 948283–948287. For ESI and crystallographic data in CIF or other electronic format see DOI: 10.1039/c3dt52140k

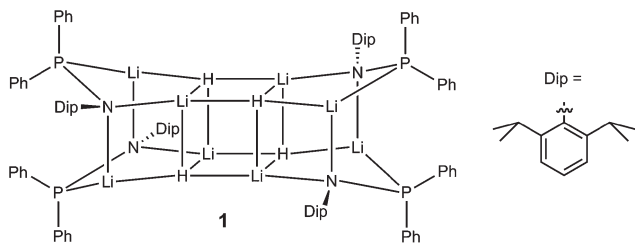


Chart 1 The phosphinoamide stabilized LiH complex 1.

$[\text{Li}(\text{THF})_4][(\text{pz})_{12}\text{Li}_{37}(\text{THF})_2\text{H}_{26}]$ (pz = 3,5-di-*tert*-butylpyrazolate).¹⁰

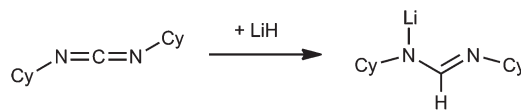
Results and discussion

Previously, we found that the hydrolithiation of benzophenone, $\text{Ph}_2\text{C}=\text{O}$, using the hydrocarbon-soluble LiH complex $[(\text{LLi})_4(\text{LiH})_4]$ **1**, affords $[(\text{Ph}_2\text{CHO})\text{Li}]_6$ ¹¹ in good yield based on the LiH content of **1**.⁹ The good isolated yield could be obtained because the product readily crystallises from the reaction solution. Here we extend our investigation of $[(\text{LLi})_4(\text{LiH})_4]$ **1** to other unsaturated organic substrates, and compare the outcomes with those of the related hydride free phosphinoamide lithium complex $[\text{LLi}]$ **2**;⁹ the latter complex being only poorly soluble in uncoordinating solvents likely due to an oligomeric or polymeric nature.⁹

The reaction of $[(\text{LLi})_4(\text{LiH})_4]$ **1** with $\text{Ph}_2\text{C}=\text{CH}_2$ or $\text{PhC}\equiv\text{CPh}$, respectively, at room temperature showed no reaction as judged by solution ^1H and $^{31}\text{P}\{^1\text{H}\}$ NMR spectroscopy. At elevated temperatures of approximately 60 °C and above, complex **1** starts to slowly decompose into poorly soluble $[\text{LLi}]$ **2** and by implication LiH, as previously reported.⁹ Product mixtures have consequently been obtained for these reactions at elevated temperatures and no reaction of the two substrates with the LiH content of **1** was apparent, though some conversion involving freshly released LiH during the decomposition cannot be excluded and would be difficult to spectroscopically detect amidst large quantities of **1** and **2**. From one of these reactions, we obtained a crop of yellow $[\text{LLi}(\text{THF})_3]$ after recrystallization from THF and both structural (see the ESI†) and spectroscopic data (see the Experimental section) are similar to those previously found for $[\text{LLi}(\text{THF})_2]$.⁹ Similarly, the reaction of **1** with 1,1-diphenylfulvene showed no reaction at room temperature and at elevated temperatures a product mixture is obtained according to ^1H and $^{31}\text{P}\{^1\text{H}\}$ NMR spectroscopy that does not permit a conclusion on the formed products.

The reactions of $[(\text{LLi})_4(\text{LiH})_4]$ **1** with *ca.* four to eight equivalents of dicyclohexylcarbodiimide (DCC) in deuterated benzene at room temperature afforded light yellow product mixtures, see the ESI for ^1H (Fig. S1†) and $^{31}\text{P}\{^1\text{H}\}$ (Fig. S2†) NMR spectra. The $^{31}\text{P}\{^1\text{H}\}$ NMR spectrum (Fig. S2†) of a typical example shows several new broadened resonances between δ 0 and 5 ppm and a broadened resonance at δ 60.8 ppm. The latter is likely attributed to a DCC donor-

stabilised phosphinoamide lithium complex, in comparison with very similar chemical shifts for THF and TMEDA adducts of $[\text{LLi}]$ **2**.⁹ Similar ^1H (Fig. S3†) and $^{31}\text{P}\{^1\text{H}\}$ (Fig. S4 and S5†) NMR spectra were found for the reaction of $[\text{LLi}]$ **2** with DCC, including very similar broad resonances around δ 0–5 ppm ($^{31}\text{P}\{^1\text{H}\}$ NMR). These suggest that phosphinoamide additions to DCC occur, likely forming substituted lithium guanidinate or phospho(v)guanidinate species. The ^1H NMR spectra for both reactions suggest that a mixture of compounds had formed and an additional strong singlet at δ 7.94 ppm (Fig. S1†) is found for the reaction involving **1**, along with partial consumption of the broad LiH resonance at δ 4.18 ppm. The former singlet is neither found in the reaction of **2** with DCC (Fig. S3†) nor in the spectrum of compound **1**⁹ and very likely shows the formamidinate¹² hydrogen in a HDCCLi fragment from the hydrolithiation of LiH fragments with DCC, see the simplified Scheme 1. The chemical shift is similar to those found for some related dicyclohexylformamidinate lithium complexes, *e.g.* δ 7.16 ppm (in C_6H_6)¹³ and δ 7.81 ppm (in THF-d_8).¹⁴



Scheme 1 Hydrolithiation of DCC.

Isolation and separation attempts by crystallization from the latter experiment afforded some small colourless needles of the formamidinate aggregate $[(\text{LSiMe}_2\text{OLi})_2(\text{HDCCLi})_2]$ **3**, see Fig. 1, that were characterized using synchrotron radiation. $[(\text{LSiMe}_2\text{OLi})_2(\text{HDCCLi})_2]$ **3**· $3\text{C}_6\text{H}_6$ crystallized with a full molecule in the asymmetric unit. The product can be described as having a central distorted Li_4 tetrahedron (dashed lines in Fig. 1) with two monoanionic substituted phosphinoamido silanolate ligands and two HDCC[−] formamidinate ligands. The silanolate groups cap two of the four Li_3 tetrahedron faces with their $\mu_3\text{-O}$ atom, and the neutral silylamido phosphine moieties coordinate to one Li centre each. The two formamidinate ligands similarly coordinate to two of the Li_3 tetrahedron faces, albeit with a $\mu_3\text{-}\kappa^1\text{N}_2\text{:}3\kappa^2\text{N}'$ coordination mode. The C–N bond lengths of the formamidinate backbone are somewhat localized and the shorter ‘amido’ C–N ones (N(5)–C(53): 1.303(2), N(6)–C(66): 1.3048(19)) belong to the $\kappa^1\text{N}$ nitrogen coordination with the shortest Li–N distances.

The product incorporates both the formamidinate ligand formed *via* hydrolithiation, see Scheme 1, and also a phosphinoamide–silicone addition product (see below, Scheme 3). Incorporation of silicone units from silicone grease polymers into organometallic and related compounds has often been described.¹⁵ Here, the addition of the phosphinoamide ligand onto a Me_2SiO moiety *via* N-attack is observed with a newly formed N–Si bond. Since complex **3** contains Me_2SiO fragments from the silicone grease polymer, some separation and crystallisation experiments were carried out in grease-free glassware. After some attempts, a small crop of crystals of

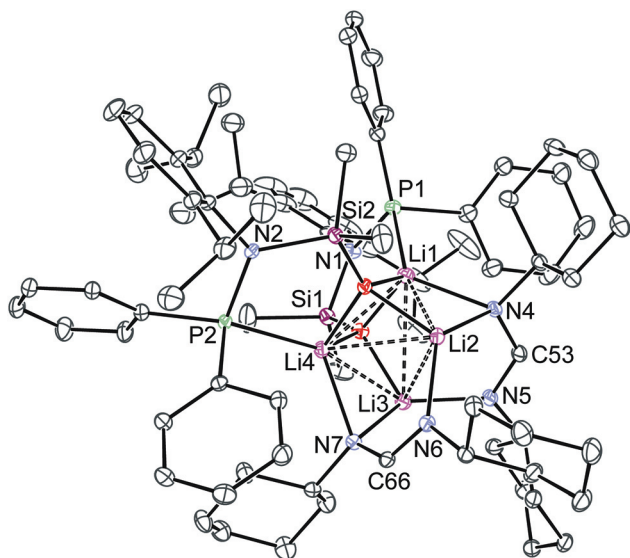


Fig. 1 Molecular structure of compound $3 \cdot 3\text{C}_6\text{H}_6$ (30% probability thermal ellipsoids). Hydrogen atoms and solvent molecules have been omitted for clarity. Selected bond lengths (Å) and angles ($^\circ$): P(1)–N(1) 1.7160(15), P(2)–N(2) 1.7148(13), P(1)–Li(1) 2.651(3), P(2)–Li(4) 2.624(3), Si(1)–O(1) 1.6005(11), Si(2)–O(2) 1.6004(11), Si(1)–N(1) 1.7807(14), Si(2)–N(2) 1.7767(13), O(1)–Li(3) 1.907(3), O(1)–Li(1) 1.921(3), O(1)–Li(4) 1.993(3), Li(1)–O(2) 1.934(3), Li(1)–N(4) 2.132(3), O(2)–Li(2) 1.896(3), O(2)–Li(4) 1.921(3), Li(2)–N(6) 1.938(3), Li(2)–N(4) 2.041(3), Li(3)–N(5) 1.952(3), Li(3)–N(7) 2.070(3), Li(4)–N(7) 2.135(3), N(4)–C(53) 1.3384(19), N(5)–C(53) 1.303(2), N(6)–C(66) 1.3048(19), N(7)–C(66) 1.338(2); P(1)–N(1)–Si(1) 116.46(8), P(2)–N(2)–Si(2) 117.49(7), Li(3)–O(1)–Li(4) 79.76(12), Li(1)–O(1)–Li(4) 81.96(11), Li(3)–O(1)–Li(1) 96.93(12), N(5)–C(53)–N(4) 125.10(13), N(6)–C(66)–N(7) 125.30(14).

known cubic $[(\text{HDCC})_6\text{Li}_8\text{O}] \mathbf{4}$,¹³ crystallised from hexane with an interstitial oxide ion, was obtained and structurally characterized, amongst some oily products that could not be purified. The central oxygen atom in **4** likely originates from trace amounts of air or moisture during recrystallization. Isolation attempts for reactions of $[\text{LLi}] \mathbf{2}$ with DCC only led to oily product mixtures that could not be separated.

The reaction of a solution of $[(\text{LLi})_4(\text{LiH})_4] \mathbf{1}$ with varying amounts of azobenzene, $\text{PhN}=\text{NPh}$, was followed by ^1H and $^{31}\text{P}\{^1\text{H}\}$ NMR over three days, see Fig. 2 for a partially assigned ^1H and $^{31}\text{P}\{^1\text{H}\}$ NMR spectrum after 16 h, and the ESI (Fig. S6–S9†). The reaction changed colour from orange *via* green to brown-yellow over the course and a product mixture was obtained that shows two main broad resonances at δ 19.7 and δ 22.5 ppm in the $^{31}\text{P}\{^1\text{H}\}$ NMR spectrum and broad resonances for the ^1Pr methyl and methine protons in the ^1H NMR spectrum. A sharp singlet at δ 4.46 (^1H NMR)¹⁶ for dihydrogen is also found. For comparison, the reaction of poorly soluble $[\text{LLi}] \mathbf{2}$ with approximately one equivalent of azobenzene is surprisingly faster and shows a very similar outcome, namely the domination of the same broad resonances in ^1H and ^{31}P NMR spectra (ESI, Fig. S10 and S11†) as compared to the same reaction involving **1**, albeit with no observed H_2 formation. The new product $[\{\text{LN}(\text{Ph})\text{N}(\text{Ph})\text{Li}\}_2] \mathbf{5}$ could be isolated as

colourless crystals from both reaction mixtures in moderate to good yields, see Fig. 3 (and see Scheme 3 below).

Isolated compound **5**, see Fig. S12 and S13† for ^1H and $^{31}\text{P}\{^1\text{H}\}$ NMR spectra, shows the broadened ^1H NMR ^1Pr resonances and the two broad ^{31}P NMR resonances at 30 $^\circ\text{C}$ previously observed from *in situ* experiments, see Fig. 2 and S8–S11,† and only shows one broad resonance at δ 21.0 ppm ($^{31}\text{P}\{^1\text{H}\}$ NMR) at 60 $^\circ\text{C}$ (Fig. S13†), and the ^1H NMR spectrum now shows one broad resonance for the ^1Pr methyl protons and a sharp septet (δ 3.44 ppm) for the ^1Pr methine protons at this temperature (Fig. S12†). One broad resonance is observed for **5** in its $^7\text{Li}\{^1\text{H}\}$ NMR spectrum. Complex **5** crystallizes with half a molecule in the asymmetric unit and shows an addition product of the phosphinoamide lithium complex and azobenzene with a newly formed P–N bond that forms a dimeric aggregate *via* Li...N interactions. The newly formed fragment is a monoanionic, chelating ligand that forms a five-membered ring with its lithium counterion. The P1–N1 bond lengths (1.5648(14) Å) suggest a predominantly iminophosphorane description and the significantly longer P1–N2 bond lengths (1.6845(14) Å) support a formulation as a single bond (see Scheme 3 below). The Li cation is three-coordinated (sum of angles 333.0(5) $^\circ$) plus shows short contacts to ^1Pr hydrogens, the shortest being *ca.* 2.55 Å. N2 is close to planar three-coordinate (sum of angles 358.3(5) $^\circ$) and is singly bonded (1.4439(19) Å) to N3 with a C–N–N–C torsion angle of *ca.* 78 $^\circ$. Recrystallization of a sample of **5** from *n*-hexane–THF afforded a crop of the structurally similar monomeric mono-THF adduct $[\text{LN}(\text{Ph})\text{N}(\text{Ph})\text{Li}(\text{THF})] \mathbf{6}$, see Fig. S15.† Complex **6** crystallizes with a full molecule in the asymmetric unit. The structure represents one-half of molecule **5** plus one THF molecule coordinating to the Li ion resulting in a three-coordinate environment. The coordination of the Li centre is somewhat asymmetric and the N–Li–O angle for the anionic hydrazide is much larger (143.9(2) $^\circ$) than that involving the neutral iminophosphorane donor (118.8(2) $^\circ$). The Li coordination is also not fully planar (sum of angles 355.6(6) $^\circ$) and is partially distorted by short contacts to ^1Pr -hydrogens; the shortest is a methine–C–H...Li contact of *ca.* 2.35 Å. The ^1H NMR spectrum of **6** shows somewhat broadened resonances comparable to **5** that sharpen at elevated temperature and show one sharp septet at 70 $^\circ\text{C}$ for the ^1Pr methine protons and a broad resonance for the ^1Pr methyl protons. The $^{31}\text{P}\{^1\text{H}\}$ NMR spectrum shows one broad resonance at δ 10.3 at 30 $^\circ\text{C}$.

To further investigate the fate of the LiH moieties in the reaction of **1** with azobenzene and the source of the dihydrogen, we tried to separate further products from the reaction mixture. We obtained yellow crystals of $[\{\text{PhN}(\text{Li})\text{N}(\text{Li})\text{Ph}\}_4] \cdot 7\text{C}_6\text{H}_6$ that were structurally characterized using synchrotron radiation, see Fig. 4. Complex **7** crystallizes with half a molecule in the asymmetric unit and consists of four $\text{PhN}(\text{Li})\text{N}(\text{Li})\text{Ph}$ units that form a central inorganic cage of four Li and eight N atoms plus four outer ‘terminal’ Li atoms. The former azobenzene N=N double bonds in **7** are now reduced to Ph–N–N–Ph^{2–} units that show long N–N single bonds of 1.466 Å and 1.469 Å. The two phenyl groups of each

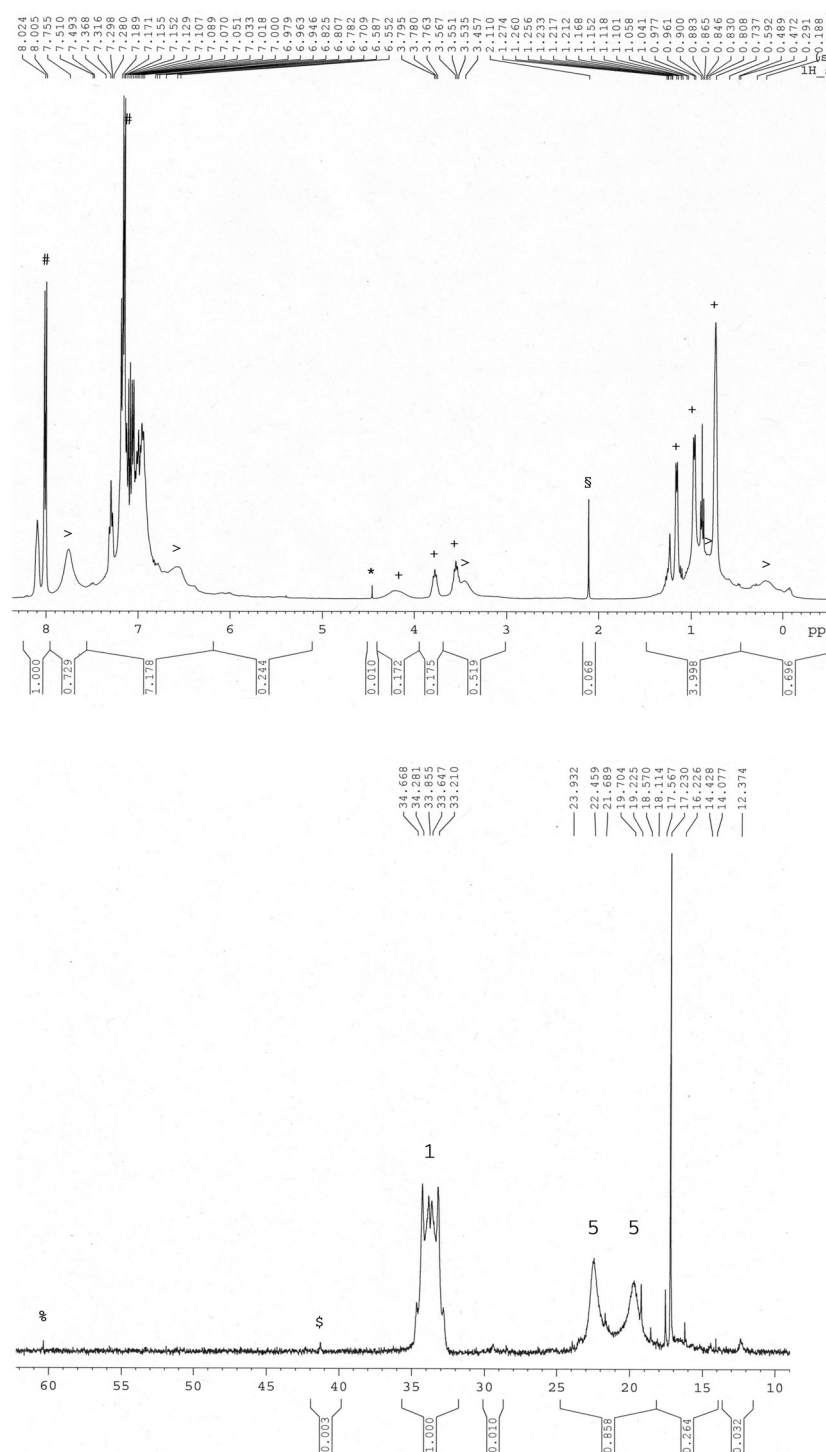


Fig. 2 ^1H NMR (400.17 MHz) spectrum (top) and $^{31}\text{P}\{^1\text{H}\}$ NMR (161.98 MHz) spectrum (bottom) of the *in situ* reaction of $[(\text{LLi})_4(\text{LiH})_4]$ **1** with $\text{PhN}=\text{NPh}$ at room temperature after ca. 16 h in deuterated benzene recorded at 303 K showing partial conversion to $[(\text{LN}(\text{Ph})\text{N}(\text{Ph})\text{Li})_2]$ **5**. ^1H : #: $\text{PhN}=\text{NPh}$ resonances; *: H_2 ; +: characteristic resonances of $[(\text{LLi})_4(\text{LiH})_4]$ **1**; >: selected resonances of $[(\text{LN}(\text{Ph})\text{N}(\text{Ph})\text{Li})_2]$ **5**; §: toluene resonance. $^{31}\text{P}\{^1\text{H}\}$: %: small amounts of a DCC donor-stabilised $\text{Ph}_2\text{PN}(\text{Dip})\text{Li}$ species; §: small amounts of $\text{Ph}_2\text{PN}(\text{H})\text{Dip}$; 1: $[(\text{LLi})_4(\text{LiH})_4]$ **1**; 5: $[(\text{LN}(\text{Ph})\text{N}(\text{Ph})\text{Li})_2]$ **5**.

substituted hydrazine-1,2-diide are twisted relative to each other around the long N–N bond by ca. 92–93°, as measured from their C–N–N–C torsion angles. The inner cage comprises four N,N,Li,N,N,Li six-membered rings and two N,Li,N,Li four-membered rings. Each N atom is connected to a phenyl group

and one neighbouring N atom, and coordinates to two Li atoms, both with different coordination environments. The four ‘inner’ Li atoms coordinate to three N atoms each and the four outer ‘terminal’ Li atoms coordinate only to one N atom, plus to two phenyl groups with short η^6 and approximate η^2

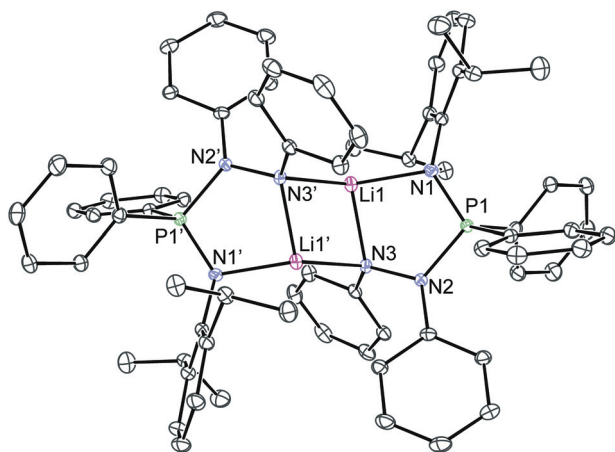


Fig. 3 Molecular structure of compound **5** (30% probability thermal ellipsoids). Hydrogen atoms have been omitted for clarity. Selected bond lengths (Å) and angles (°): P(1)–N(1) 1.5648(14), P(1)–N(2) 1.6845(14), N(1)–Li(1) 1.943(3), Li(1)–N(3) 2.020(3), Li(1)–N(3') 2.035(3), N(2)–N(3) 1.4439(19), N(3)–Li(1') 2.035(3); N(1)–P(1)–N(2) 106.95(7), N(3)–N(2)–P(1) 115.49(10), N(1)–Li(1)–N(3) 90.35(13), N(1)–Li(1)–N(3') 134.78(18), N(3)–Li(1)–N(3') 107.89(14); symmetry transformations: '1 –x + 1, –y, –z.

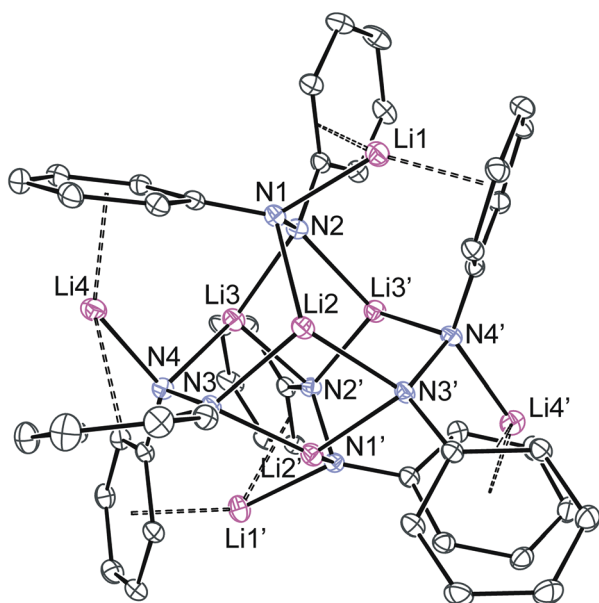


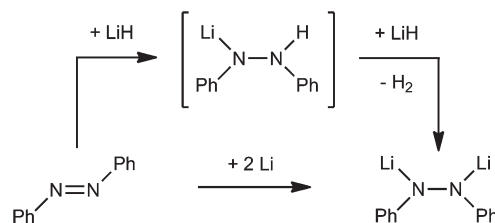
Fig. 4 Molecular structure of compound **7** (30% probability thermal ellipsoids). Hydrogen atoms and solvent molecules have been omitted for clarity. Selected bond lengths (Å) and angles (°): N(1)–N(2) 1.466(2), N(3)–N(4) 1.469(2), N(1)–Li(1) 1.992(4), N(1)–Li(2) 2.023(4), N(2)–Li(3) 2.018(4), N(2)–Li(3') 2.052(4), Li(2)–N(3') 2.022(4), Li(2)–N(3) 2.048(3), N(3)–Li(2') 2.022(4), Li(3)–N(4) 1.998(4), Li(3)–N(2') 2.052(4), N(4)–Li(4) 1.984(4), N(2)–N(1)–Li(1) 92.47(14), N(2)–N(1)–Li(2) 100.11(14), N(1)–N(2)–Li(3) 105.54(14), Li(1)–N(1)–Li(2) 101.06(15), N(1)–N(2)–Li(3') 122.46(14), Li(3)–N(2)–Li(3') 74.24(15); symmetry transformation: '1 –x, y, –z + 1/2.

coordination, respectively. The Li $\cdots\eta^6$ -Ph(centroid) distances measure *ca.* 2.014 Å and 2.049 Å, and the Li $\cdots\eta^2$ -Ph(C–C midpoint) distances are *ca.* 2.375 Å and 2.454 Å, respectively. In

addition, these outer Li atoms further show one contact each to lattice benzene molecules (not shown in Fig. 4), the shortest being either a η^1 -C₆H₆ contact of *ca.* 3.052 Å, or a η^2 -C₆H₆ contact of *ca.* 3.410 Å to the C–C midpoint. The product is a tetrameric PhN(Li)–N(Li)Ph aggregate from the formal addition of zero-valent lithium to azobenzene.

In order to obtain compound **7** for additional spectroscopic data, we attempted a synthesis from an excess of lithium metal and azobenzene. A slurry of an excess of lithium metal in benzene was treated with azobenzene at room temperature and within minutes to one hour, the red-orange colour from azobenzene faded to a more yellow reaction mixture. After several hours of stirring, the mixture was filtered and concentration of the yellow solution afforded crystalline [PhN(Li)–N(Li)Ph]₄·7·C₆H₆ in low to moderate isolated yield. The identity of the crystalline material was confirmed by a unit cell determination using synchrotron radiation and compared to the previously obtained crystals using **1**. Once crystallised, which likely happens during the reduction reaction, the yellow compound is only sparingly soluble in hot benzene. ¹H and ¹³C{¹H} NMR spectra of this compound as a yellow solution/slurry recorded at elevated temperature in deuterated benzene are not very informative and only display weak and very broad resonances characteristic for aromatic groups. The addition of some THF led to dissolution, but is accompanied with a colour change to yellow-green brown and further only shows very broad and overlapping ¹H, ⁷Li{¹H} and ¹³C{¹H} NMR resonances in the respective spectra.

The reactivity of the LiH units from **1** and metallic Li, respectively, towards azobenzene is summarized in Scheme 2 in a simplified form. Hydrolithiation of soluble LiH across the N=N double bond of azobenzene is expected to furnish a monolithiated hydrazine derivative with newly formed protic hydrogen with umpolung of its charge. From the s-block of the periodic table, there is precedent for this reactivity in the form of a stable analogous β -diketiminate magnesium fragment [LMg⁺ \leftrightarrow Li⁺] formed *via* the comparable hydromagnesiation reaction.¹⁷ This intermediate was not observed in the Li case and likely rapidly reacts with further LiH units under hydrogen evolution, as observed by ¹H NMR spectroscopy, and forms the isolated dilithium hydrazine-1,2-diide product **7**. This represents a complete and facile low temperature hydrogen generation from lithium hydride without protic reagents. Alternatively, the hydrazine-1,2-diide product **7** was prepared by direct reduction of azobenzene with two equivalents of lithium metal. Similarly, a β -diketiminate stabilized dimeric



Scheme 2 Azobenzene reaction with LiH fragments and Li metal.

magnesium(i) compound adds the magnesium fragments across the N=N double bond of azobenzene, $[\text{LMg}^{\bullet} \leftrightarrow \text{Li}^{\bullet}]$, though the Mg^{2+} coordination to the resulting hydrazine-1,2-diide ligand involves some dearomatization of the phenyl rings and it thus acts as a bis-azaallyl ligand, and shows a shorter N–N single bond (1.424(2) Å).¹⁷

The stabilizing phosphinoamide ligand $[\text{Ph}_2\text{PNDip}]^{\bullet-}$, $\text{Li}^{\bullet-}$, in **1** and **2** was found to react with several of the investigated substrates, and addition products with dimethylsilicone (3) and azobenzene (5) units have been structurally characterized. The different reactivity is shown in Scheme 3. The phosphinoamide reaction with the dimethylsilicone units proceeds with an N-attack on the Si centre and forms a silanolate with a neutral donating amidophosphine (P^{III}) centre (a). In contrast, the phosphinoamide addition onto azobenzene proceeds with P-attack to yield a chelating hydrazido ligand with a σ^4, λ^5 phosphorane (P^{V}) centre plus a neutral donating imino nitrogen centre (b). The first reaction is an addition reaction without formal change of redox states and the latter involves a redox reaction between the P centre and the azobenzene- N_2 core.

This difference in reactivity can be explained with the ‘hard and soft (Lewis) acid and base concept’. The hard amide nitrogen atom attacks the hard silicon Si^{IV} centre (Scheme 3(a)) and the softer phosphine attacks the softer electrophile azobenzene (b). Although a likely explanation, steric reasons for this difference cannot completely be excluded. Structural data on phosphinoamide complexes strongly favour a formulation with the negative charge located on the more electronegative N atom,^{8,18} see Chart 2A, and not on the P atom, Chart 2B. Previously it has been pointed out that phosphinoamides (such as in form A) rather react as iminophosphides (as in B) towards electrophiles such as MeI or Ph_2PCl and P-substituted products are formed.^{8,18} These electrophiles can be regarded

as relatively soft and are thus attacked by the softer nucleophilic site of the anion.

Conclusions

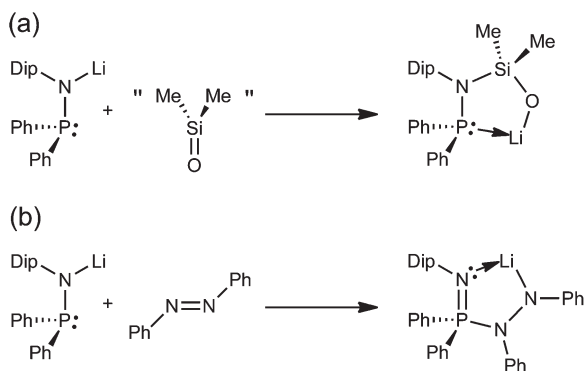
The LiH moieties in the hydrocarbon-soluble LiH complex **1** can undergo hydrolithiation reactions with some heteroatom-containing unsaturated organic substrates, such as benzophenone,⁹ dicyclohexylcarbodiimide (DCC) and azobenzene. For DCC, fragments with the expected lithium formamidinate have been found while for azobenzene, a hydrolithiation leads to an umpolung reaction yielding a protic NH that reacts with a further LiH to produce H_2 . This represents a facile low temperature hydrogen liberation from LiH fragments without the use of protic reagents (though a protic species is formed as an intermediate) or high temperature. No reactions of **1** with 1,1-diphenylethylene, diphenylacetylene, and 1,1-diphenylfulvene, respectively, have been observed at room temperature. The hydrometalation reactivity is comparable to that of related s-block β -diketiminato stabilized $\text{CaH}^{2,19}$ and $\text{MgH}^{2,17,20}$ fragments, though the latter examples appear both more reactive and thermally robust; the former observation is likely due to the capacity of the divalent metal ions to better activate the substrate and likely not due to differences in ionic character of the hydride moieties.

It has furthermore been found that several of the investigated reactions of **1** herein were accompanied by reactions of the stabilizing phosphinoamide ligand with the respective substrates. The phosphinoamide $[\text{Ph}_2\text{PNDip}]^{\bullet-}$ was found to react with azobenzene *via* attack of the P atom, and with a dimethylsilicone moiety from silicone grease *via* attack of the N atom. This differing reactivity can be explained by the hard and soft acid base approach, though steric reasons cannot be excluded. The phosphinoamide moiety can consequently not be considered an inert spectator ligand for these reactivity studies and the introduction and development of more inert stabilizing ligands are required to further advance the chemistry of group 1 metal hydride complexes. To this end, the recent introduction of large pyrazolato-stabilised LiH clusters¹⁰ can be a suitable approach to suppress these types of side-reactions.

Experimental section

General considerations

All manipulations were carried out using standard Schlenk and glove box techniques under an atmosphere of high purity dinitrogen. Benzene, toluene, tetrahydrofuran and hexane were dried and distilled over molten potassium. ^1H , $^7\text{Li}\{^1\text{H}\}$, $^{13}\text{C}\{^1\text{H}\}$, and $^{31}\text{P}\{^1\text{H}\}$ NMR spectra were recorded on a Bruker DPX 300 or Bruker Avance 400 spectrometer in deuterated benzene and were referenced to the residual ^1H or $^{13}\text{C}\{^1\text{H}\}$ resonances of the solvent used, or external aqueous LiCl, or H_3PO_4 solutions, respectively. IR spectra were recorded using a Perkin Elmer RXI FT-IR spectrometer as Nujol mulls between



Scheme 3 Silicone and azobenzene addition onto a lithium phosphinoamide.

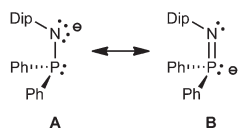


Chart 2 Phosphinoamide and iminophosphide mesomeric forms of $\text{Li}^{\bullet-}$.

NaCl plates, or on solids protected with a thin layer of nujol using an Agilent Cary 630 ATR FTIR spectrometer. The solid state mass spectrum was recorded using an Agilent 5975C inert MSD with triple-axis detector and SIS direct insertion probe. Melting points were determined in sealed glass capillaries under dinitrogen and are uncorrected. Elemental analyses were performed by the Elemental Analysis Service at London Metropolitan University. $[(\text{LLi})_4(\text{LiH})_4]$ **1** and $[\text{LLi}]$ **2**⁹ were prepared according to literature procedures. All other reagents were used as received (Aldrich Chemical Company). Abbreviations: br = broad, vbr = very broad, m = multiplet. NMR scale reactions were typically carried out on ca. 20 mg samples in 5 mm NMR tubes with J. Young stopcock in dried deuterated benzene (ca. 0.55 mL), followed by ^1H and $^{31}\text{P}\{^1\text{H}\}$ NMR spectroscopy, and are described in the main text. ^1H and $^{31}\text{P}\{^1\text{H}\}$ NMR spectra of reactions of $[(\text{LLi})_4(\text{LiH})_4]$ **1**, and $[\text{LLi}]$ **2**, with DCC and $\text{PhN}=\text{NPh}$, respectively, are given in the ESI.†

Spectroscopic data for $[\text{LLi}(\text{THF})_3]$

The title compound was obtained by recrystallization of a $[\text{LLi}]$ containing sample from THF. The spectroscopic data are similar to that previously reported for $[\text{LLi}(\text{THF})_2]$.⁹ Yellow crystals; mp: 97–100 °C; ^1H NMR (C_6D_6 , 400.1 MHz, 303 K): δ 1.22 (m, 12H, $\text{THF-OCH}_2\text{CH}_2$), 1.31 (d, $J_{\text{H-H}} = 6.8$ Hz, 12H, $\text{CH}(\text{CH}_3)_2$), 3.18 (m, 12H, $\text{THF-OCH}_2\text{CH}_2$), 4.16 (sept, br, $J_{\text{H-H}} \approx 6.8$ Hz, 2H, $\text{CH}(\text{CH}_3)_2$), 6.95–7.29 (m, 9H, Ar-H), 7.75–7.85 (m, 4H, Ar-H); ^7Li NMR (C_6D_6 , 155.5 MHz, 303 K): δ 0.77 (s); $^{13}\text{C}\{^1\text{H}\}$ NMR (C_6D_6 , 100.6 MHz, 303 K): δ 24.4–24.5 ($\text{CH}(\text{CH}_3)_2$, $\text{THF-OCH}_2\text{CH}_2$), 28.0 (d, $J_{\text{C-P}} = 4.8$ Hz, $\text{CH}(\text{CH}_3)_2$), 68.2 ($\text{THF-OCH}_2\text{CH}_2$), 118.7 (d, not well resolved, Ar-C), 123.5 (d, $J_{\text{C-P}} = 1.7$ Hz, Ar-C), 126.6 (Ar-C), 127.9 (d, $J_{\text{C-P}} = 4.5$ Hz, Ar-C), 131.6 (d, $J_{\text{C-P}} = 18.8$ Hz, Ar-C), 144.6 (d, $J_{\text{C-P}} = 5.4$ Hz, Ar-C), 152.9 (d, br, $J_{\text{C-P}} \approx 30$ Hz, Ar-C), 156.2 (d, $J_{\text{C-P}} \approx 19$ Hz, Ar-C); $^{31}\text{P}\{^1\text{H}\}$ NMR (C_6D_6 , 162.0, 303 K): δ 60.5 (br); IR (nujol), $\tilde{\nu}/\text{cm}^{-1}$: 1583m, 1460s, 1432m, 1417m, 1375m, 1366m, 1307s, 1253m, 1231s, 1185s, 1102m, 1075m, 1045s, 911s, 822m, 778s, 737s, 699s, 680m, 574 m.

$[(\text{LSiMe}_2\text{OLi})_2(\text{HDCCLi})_2]$ **3**: $3\text{C}_6\text{H}_6$ and $[(\text{HDCC})_6\text{Li}_8\text{O}]$ **4**¹³

The reaction of $[(\text{LLi})_4(\text{LiH})_4]$ **1** with DCC at room temperature led to oily product mixtures that could not be separated. ^1H and $^{31}\text{P}\{^1\text{H}\}$ NMR spectra for the *in situ* reaction can be found in the ESI (Fig. S1 and S2†) plus those of the related reaction of $[\text{LLi}]$ **2** with DCC (Fig. S3–5†). Separation attempts did lead to small amounts of crystals of the title compounds that were structurally characterised only after incorporation of silicone grease (**3**) or traces of air or moisture (**4**); further details are described in the main text.

$[\{\text{LN}(\text{Ph})\text{N}(\text{Ph})\text{Li}\}_2]$ **5**

The title compound was formed and isolated from reactions involving $[(\text{LLi})_4(\text{LiH})_4]$ **1**, and $[\text{LLi}]$ **2** with azobenzene, respectively, see main text. For a preparative scale:

Azobenzene (0.245 g, 1.346 mmol, 1.03 eq.) was added to a cooled (–80 °C) fine slurry of $[\text{LLi}]$ **2** (0.48 g, 1.306 mmol) in toluene (20 mL). The reaction was stirred briefly at this

temperature, then slowly warmed to room temperature and stirred overnight. An off-white crystalline precipitate of **5** had formed which was filtered off. Concentration of the yellow-brown filtrate to ca. 10 mL and cooling to 4 °C afforded a second crop of colourless crystals of **5**, further concentration to ca. 4 mL and cooling to 4 °C afforded a small third crop. Obtained crops were washed with a small amount of *n*-hexane (ca. 3–4 mL) and dried under vacuum. Yield: 0.42 g (0.382 mmol, 58%); mp: decomposition, above ca. 210 °C gradually more yellow, then brown; fully decomposed at around 240 °C; ^1H NMR (C_6D_6 , 300.1 MHz, 303 K): δ 0.25 (vbr, 12H, $\text{CH}(\text{CH}_3)_2$), 0.90 (vbr, 12H, $\text{CH}(\text{CH}_3)_2$), 3.47 (br, 4H, $\text{CH}(\text{CH}_3)_2$), 6.47–7.33 (m, 38H, Ar-H), 7.67–7.83 (br, 8H, Ar-H); ^1H NMR (C_6D_6 , 300.1 MHz, 333 K): δ 0.70 (br, 24H, $\text{CH}(\text{CH}_3)_2$), 3.44 (sept, $J_{\text{H-H}} \approx 6.8$ Hz, 4H, $\text{CH}(\text{CH}_3)_2$), 6.54 (t, br, $J_{\text{H-H}} \approx 7.2$ Hz, 4H, Ar-H), 6.72 (t, vbr, 4H, Ar-H), 6.82–7.31 (m, 30H, Ar-H), 7.74 (dd, br, $J_{\text{H-H}} \approx 10.8$, 7.8 Hz, 8H, Ar-H); ^7Li NMR (C_6D_6 , 155.5 MHz, 303 K): δ 3.3 (br); $^{13}\text{C}\{^1\text{H}\}$ NMR (C_6D_6 , 75.5 MHz, 333 K): δ 24.4 (vbr, $\text{CH}(\text{CH}_3)_2$), 28.5 ($\text{CH}(\text{CH}_3)_2$), 112.8 (br, Ar-C), 114.9 (Ar-C), 119.8 (d, not well resolved, Ar-C), 121.3 (Ar-C), 122.8 (d, $J_{\text{C-P}} = 3.5$ Hz, Ar-C), 123.9 (d, $J_{\text{C-P}} = 2.4$ Hz, Ar-C), 128.3 (Ar-C), 128.7 (Ar-C), 130.0 (Ar-C), 131.3 (br, Ar-C), 133.0 (m, br, overlapping Ar-C), 141.3 (Ar-C), 145.3 (d, $J_{\text{C-P}} = 6.3$ Hz, Ar-C), 147.2 (d, $J_{\text{C-P}} = 19.2$ Hz, Ar-C), 160.9 (Ar-C); $^{31}\text{P}\{^1\text{H}\}$ NMR (C_6D_6 , 162.0, 303 K): δ 19.7 (vbr), 22.5 (vbr); $^{31}\text{P}\{^1\text{H}\}$ NMR (C_6D_6 , 121.5 333 K): δ 21.0 (br); IR (nujol), $\tilde{\nu}/\text{cm}^{-1}$: 1594m, 1479m, 1460s, 1437s, 1376s, 1332m, 1298m, 1280m, 1228s, 1214m, 1111m, 1052m, 1027s, 944m, 812m, 778m, 750s, 721m, 690m; elemental analysis (%) for $\text{C}_{72}\text{H}_{74}\text{Li}_2\text{N}_6\text{P}_2$ (1099.23 g mol^{–1}): calcd: C 78.67, H 6.79, N 7.65; found: C 78.63, H 6.68, N 7.55.

Spectroscopic data for $[\text{LN}(\text{Ph})\text{N}(\text{Ph})\text{Li}(\text{THF})]$ **6**

Colourless crystals of the title compound were obtained by recrystallizing a sample of **5** from hexane–THF. ^1H NMR (C_6D_6 , 300.1 MHz, 303 K): δ 0.85 (vbr, 6H, $\text{CH}(\text{CH}_3)_2$), 1.14 (vbr, 6H, $\text{CH}(\text{CH}_3)_2$), 1.18 (m, 4H, $\text{THF-OCH}_2\text{CH}_2$), 3.36 (m, 4H, $\text{THF-OCH}_2\text{CH}_2$), 3.64 (sept, br, 2H, $\text{CH}(\text{CH}_3)_2$), 6.49–7.82 (m, 21H, Ar-H), 8.31 (vbr, 2H, Ar-H); ^1H NMR (C_6D_6 , 300.1 MHz, 343 K): δ 0.96 (br, 12H, $\text{CH}(\text{CH}_3)_2$), 1.33 (m, 4H, $\text{THF-OCH}_2\text{CH}_2$), 3.47 (m, 4H, $\text{THF-OCH}_2\text{CH}_2$), 3.65 (sept, $J_{\text{H-H}} = 6.8$ Hz, 2H, $\text{CH}(\text{CH}_3)_2$), 6.43–8.10 (m, 23H, Ar-H); ^7Li NMR (C_6D_6 , 155.5 MHz, 303 K): δ 2.6 (m); $^{13}\text{C}\{^1\text{H}\}$ NMR (C_6D_6 , 75.5 MHz, 343 K): δ 24.1 ($\text{CH}(\text{CH}_3)_2$), 25.4 ($\text{THF-OCH}_2\text{CH}_2$), 28.3 ($\text{CH}(\text{CH}_3)_2$), 68.6 ($\text{THF-OCH}_2\text{CH}_2$), 112.1 (br, Ar-C), 112.7 (br, Ar-C), 121.5–122.3 (m, overlapping resonances, Ar-C), 123.6 (Ar-C), 128.1 (partially hidden by solvent resonances, Ar-C), 129.0 (Ar-C), 131.2 (d, $J_{\text{C-P}} = 2.2$ Hz, Ar-C), 133.2 (d, $J_{\text{C-P}} = 8.8$ Hz, Ar-C), 144.0–144.4 (m, overlapping resonances, Ar-C), 146.7 (d, $J_{\text{C-P}} = 10.1$ Hz, Ar-C), 160.0 (br, Ar-C); $^{31}\text{P}\{^1\text{H}\}$ NMR (C_6D_6 , 162.0, 303 K): δ 10.3 (br).

$[\{\text{PhN}(\text{Li})\text{-N}(\text{Li})\text{Ph}\}_4]$ **7**: $6\text{C}_6\text{H}_6$

Yellow, rod to needle-like crystals of the title compound were obtained from the reaction of LiH complex **1** with PhNNPh , alongside $[\{\text{LN}(\text{Ph})\text{N}(\text{Ph})\text{Li}\}_2]$ **5**, see main text.

Route to material for spectroscopic data: Azobenzene (0.23 g, 1.26 mmol) was added to a suspension of finely divided and washed (*n*-hexane, 2 × 15–20 mL) Li metal (dispersion in mineral oil, high sodium, excess, *ca.* 60–100 mgs) in benzene (15 mL) at room temperature. Within several minutes, the colour changed from red-orange to largely yellow. The mixture was stirred for six hours and a yellow precipitate formed alongside residual fine-divided Li. The reaction mixture was brought to 70 °C for 30 min to allow more product to dissolve and was filtered at that temperature. Concentration to *ca.* 6 mL and cooling to 12 °C afforded a crop of yellow rod to needle-like crystals of $[\{\text{PhN}(\text{Li})\text{-N}(\text{Li})\text{Ph}\}_4] \cdot 7\text{-C}_6\text{H}_6$. Inspecting the material under a microscope showed that only one crystal form was present. A determination of the unit cell dimensions on these crystals using synchrotron radiation matched those obtained from the reaction using **1**. Two further extractions of the reaction residue with benzene (20 mL) at 70 °C afforded a yellow solution that, after concentration and cooling, afforded further crops. The yield seems to be largely limited by the low solubility once the product has crystallized, and by separation issues from metallic lithium. The combined solids were dried under vacuum at *ca.* 40 °C to afford $[\{\text{PhN}(\text{Li})\text{-N}(\text{Li})\text{Ph}\}_4] \cdot x\text{-C}_6\text{H}_6$ ($x \approx 2$). NMR spectroscopy suggests that not all six benzene molecules per formula unit were removed upon drying under vacuum. Yield: *ca.* 70 mg (*ca.* 23%); mp: slow colour change towards brown above *ca.* 240 °C, rapid decomposition above *ca.* 260 °C; ^1H NMR (C_6D_6 , 300.1 MHz, 338 K): δ *ca.* 6.12, 6.50, 6.90 (all v br, Ph-*H*); $^{13}\text{C}\{^1\text{H}\}$ NMR (C_6D_6 , 75.5 MHz, 338 K): δ *ca.* 110, 114.2, 128.5 (all br, Ph-*C*); Addition of a small amount of THF to this sample led to the dissolution of the yellow crystalline material, but also to a colour change to yellow-green brown. ^1H NMR (C_6D_6 -THF (*ca.* 10 : 1), 300.1 MHz, 300 K): δ *ca.* 6.36, 6.52, 7.14

(all v br, Ph-*H*); ^7Li NMR (C_6D_6 -THF (*ca.* 10 : 1), 155.5 MHz, 300 K): δ *ca.* 0.4–1.4 (br m); $^{13}\text{C}\{^1\text{H}\}$ NMR (C_6D_6 -THF (*ca.* 10 : 1), 100.6 MHz, 300 K): δ *ca.* 108, 114, 130 (all v br, Ph-*C*); IR (nujol), $\tilde{\nu}/\text{cm}^{-1}$: 1569s, 1543m, 1533m, 1464s, 1320m, 1286s, 1256s, 1164m, 1151m, 1070m, 1017m, 974m, 835m, 864m, 835m, 813m, 775m, 759s, 742s, 688s; EI-MS (solid state, 70 eV) m/z (%): 182.1 (27, PhN_2Ph^+), 105.0 (13, PhN_2^+), 93 (21, PhNH_2^+), 77.0 (100, Ph^+).

X-ray crystallography

Suitable crystals were mounted in silicone oil and were either measured using an Oxford Xcalibur Gemini Ultra diffractometer (**6**) with $\text{MoK}\alpha$ radiation ($\lambda = 0.71073 \text{ \AA}$), or at the MX1 beamline at the Australian Synchrotron using synchrotron radiation with a wavelength close to $\text{MoK}\alpha$ radiation. All structures were refined using SHELX.²¹ All non-hydrogen atoms were refined anisotropically. Semi-empirical (multi-scan) absorption corrections were performed on all datasets. In the structure of $[\text{LLi}(\text{THF})_3]$ (see the ESI†), one coordinated THF molecule (O2) was disordered and successfully modelled with two positions (*ca.* 65% and 35% parts) for C29–C32. The three benzene molecules in $[(\text{LSiMe}_2\text{OLi})_2(\text{HDCCLi})_2] \cdot 3\text{-C}_6\text{H}_6$ were poorly ordered and have been refined using geometry restraints. The Dip group on N1 shows a relatively large liberation mode that leads to some Level B alerts in cif-check. The relatively low data completeness of 95.7% (at 25.00° theta) for $[\{\text{LN}(\text{Ph})\text{N}(\text{Ph})\text{Li}\}_2]$ **5** is due to the experimental setup at the synchrotron at the time of collection and only one phi scan was collected. Refinement details are summarized in Table 1 and further information can be found in the crystallographic information files. CCDC 948283–948287 contains the supplementary crystallographic data for this paper.

Table 1 Crystallographic data

Compound reference	LLi(THF) ₃	3·3C ₆ H ₆	5	6	7·6C ₆ H ₆
Chemical formula	C ₃₆ H ₅₁ LiNO ₃ P	C ₉₆ H ₁₃₀ Li ₄ N ₆ O ₂ P ₂ Si ₂	C ₇₂ H ₇₄ Li ₂ N ₆ P ₂	C ₄₀ H ₄₅ LiN ₃ OP	C ₈₄ H ₇₆ Li ₈ N ₈
Formula mass	583.69	1545.94	1099.19	621.70	1253.05
Crystal system	Monoclinic	Monoclinic	Monoclinic	Triclinic	Monoclinic
<i>a</i> /Å	10.393(2)	14.003(3)	14.562(3)	10.0694(8)	33.502(7)
<i>b</i> /Å	18.147(4)	22.742(5)	14.076(3)	12.8595(9)	9.7280(19)
<i>c</i> /Å	18.322(4)	28.741(6)	14.694(3)	13.9119(11)	25.910(5)
α /°	90.00	90.00	90.00	88.050(6)	90.00
β /°	102.61(3)	94.69(3)	91.81(3)	75.353(7)	124.53(3)
γ /°	90.00	90.00	90.00	83.371(6)	90.00
Unit cell volume/Å ³	3372.2(12)	9122(3)	3010.4(10)	1731.2(2)	6956(2)
Temperature/K	100(2)	100(2)	100(2)	123(2)	100(2)
Space group	<i>P</i> 2 ₁ / <i>n</i>	<i>P</i> 2 ₁ / <i>c</i>	<i>P</i> 2 ₁ / <i>n</i>	<i>P</i>	<i>C</i> 2/ <i>c</i>
No. of formula units per unit cell, <i>Z</i>	4	4	2	2	4
Radiation type	Synchrotron	Synchrotron	Synchrotron	MoK α	Synchrotron
No. of reflections measured	29 970	122 779	27 531	11 808	30 168
No. of independent reflections	8381	23 130	7161	6783	8348
<i>R</i> _{int}	0.0511	0.0545	0.0698	0.0387	0.0682
Final <i>R</i> ₁ values (<i>I</i> > 2σ(<i>I</i>))	0.0466	0.0652	0.0486	0.0546	0.0630
Final w <i>R</i> (<i>F</i> ²) values (<i>I</i> > 2σ(<i>I</i>))	0.1146	0.1720	0.1172	0.1096	0.1543
Final <i>R</i> ₁ values (all data)	0.0586	0.0774	0.0685	0.0844	0.0941
Final w <i>R</i> (<i>F</i> ²) values (all data)	0.1234	0.1827	0.1275	0.1248	0.1741
Goodness of fit on <i>F</i> ²	1.038	1.025	1.023	1.017	1.023
CCDC number	948283	948284	948285	948286	948287

Acknowledgements

A.S. is grateful to the Australian Research Council for support and a fellowship. Part of this research was undertaken on the MX1 beamline at the Australian Synchrotron, Victoria, Australia.

References

- 1 N. N. Greenwood and A. Earnshaw, *Chemistry of the Elements*, Elsevier, Oxford, 2nd edn, 1997.
- 2 S. Harder, *Chem. Commun.*, 2012, **48**, 11165; and references therein.
- 3 S. Aldridge and A. J. Downs, *Chem. Rev.*, 2001, **101**, 3305.
- 4 M. J. Michalczyk, *Organometallics*, 1992, **11**, 2307.
- 5 J. Haywood and A. E. H. Wheatley, *Dalton Trans.*, 2008, 3378.
- 6 (a) S. R. Boss, M. P. Coles, V. Eyre-Brook, F. Garcia, R. Haigh, P. B. Hitchcock, M. McPartlin, J. V. Morey, H. Naka, P. R. Raithby, H. A. Sparkes, C. W. Tate and A. E. H. Wheatley, *Dalton Trans.*, 2006, 5574; (b) S. R. Boss, M. P. Coles, R. Haigh, P. B. Hitchcock, R. Snaith and A. E. H. Wheatley, *Angew. Chem., Int. Ed.*, 2003, **42**, 5593; (c) D. R. Armstrong, R. P. Davies, W. Clegg, S. T. Liddle, D. J. Linton, P. Schooler, R. Snaith and A. E. H. Wheatley, *Phosphorus, Sulfur Silicon Relat. Elem.*, 2001, **168**, 93; (d) D. R. Armstrong, W. Clegg, R. P. Davies, S. T. Liddle, D. J. Linton, P. R. Raithby, R. Snaith and A. E. H. Wheatley, *Angew. Chem., Int. Ed.*, 1999, **38**, 3367.
- 7 D. Hoffmann, T. Kottke, R. J. Lagow and R. D. Thomas, *Angew. Chem., Int. Ed.*, 1998, **37**, 1537.
- 8 Z. Fei and P. Dyson, *Coord. Chem. Rev.*, 2005, **249**, 2056.
- 9 A. Stasch, *Angew. Chem., Int. Ed.*, 2012, **51**, 1930.
- 10 A. Stasch, *Angew. Chem., Int. Ed.*, 2014, **53**, 1338.
- 11 C. Frenzel and E. Hey-Hawkins, *Phosphorus, Sulfur Silicon Relat. Elem.*, 1998, **143**, 1.
- 12 P. C. Junk and M. L. Cole, *Chem. Commun.*, 2007, 1579.
- 13 E. Iravani and B. Neumüller, *Organometallics*, 2005, **24**, 842.
- 14 C. Cornelißen, G. Erker, G. Kehr and R. Fröhlich, *Z. Naturforsch., B: Chem. Sci.*, 2004, **59**, 1246.
- 15 I. Haiduc, *Organometallics*, 2004, **23**, 3.
- 16 G. R. Fulmer, A. J. M. Miller, N. H. Sherden, H. E. Gottlieb, A. Nudelman, B. M. Stoltz, J. E. Bercaw and K. I. Goldberg, *Organometallics*, 2010, **29**, 2176.
- 17 S. J. Bonyhady, S. P. Green, C. Jones, S. Nembenna and A. Stasch, *Angew. Chem., Int. Ed.*, 2009, **48**, 2973.
- 18 Z. Fei, R. Scopelliti and P. Dyson, *Inorg. Chem.*, 2003, **42**, 2125.
- 19 (a) J. Spielmann, F. Buch and S. Harder, *Angew. Chem., Int. Ed.*, 2008, **47**, 9434; (b) J. Spielmann and S. Harder, *Chem.-Eur. J.*, 2007, **13**, 8928; (c) S. Harder and J. Brettar, *Angew. Chem., Int. Ed.*, 2006, **45**, 3474.
- 20 (a) J. Intemann, J. Spielmann, P. Sirsch and S. Harder, *Chem.-Eur. J.*, 2013, **19**, 8478; (b) C. Jones, S. J. Bonyhady, S. Nembenna and A. Stasch, *Eur. J. Inorg. Chem.*, 2012, 2596; (c) M. S. Hill, M. Hodgson, D. J. Liptrot and M. F. Mahon, *Dalton Trans.*, 2011, **40**, 12500; (d) M. Arrowsmith, M. S. Hill, T. Hadlington, G. Kociok-Köhn and C. Weetman, *Organometallics*, 2011, **30**, 5556; (e) J. Spielmann and S. Harder, *Dalton Trans.*, 2011, **40**, 8314; (f) M. S. Hill, G. Kociok-Köhn, D. J. MacDougall, M. F. Mahon and C. Weetman, *Dalton Trans.*, 2011, **40**, 7783; (g) S. Harder, J. Spielmann, J. Intemann and H. Bandmann, *Angew. Chem., Int. Ed.*, 2011, **50**, 4156; (h) M. S. Hill, D. J. MacDougall and M. F. Mahon, *Dalton Trans.*, 2010, **39**, 11129; (i) J. Spielmann, D. F.-J. Piesik and S. Harder, *Chem.-Eur. J.*, 2010, **16**, 8307; (j) S. J. Bonyhady, C. Jones, S. Nembenna, A. Stasch, A. J. Edwards and G. J. McIntyre, *Chem.-Eur. J.*, 2010, **16**, 938; (k) S. J. Bonyhady, D. Collis, G. Frenking, N. Holzmann, C. Jones and A. Stasch, *Nat. Chem.*, 2010, **2**, 865; (l) J. Spielmann, M. Bolte and S. Harder, *Chem. Commun.*, 2009, 6934; (m) S. P. Green, C. Jones and A. Stasch, *Angew. Chem., Int. Ed.*, 2008, **47**, 9079.
- 21 G. M. Sheldrick, *Acta Crystallogr., Sect. A: Fundam. Crystallogr.*, 2008, **64**, 112.